Functional characterization of novel ABCB6 mutations and their clinical implications in familial pseudohyperkalemia

Immacolata Andolfo,[1,2] Roberta Russo,[1,2] Francesco Manna,[1,2] Gianluca De Rosa,[1,2] Antonella Gambale,[1,2] Soha Zouwail,[3] Nicola Detta,[2] Catia Lo Pardo,[4] Seth L. Alper,[5] Carlo Brugnara,[6] Alok K. Sharma,[5] Lucia De Franceschi,[7] and Achille Iolascon[1,2]

[1]Department of Molecular Medicine and Medical Biotechnologies, "Federico II" University of Naples, Italy; [2]CEINGE, Biotecnologie Avanzate, Naples, Italy; [3]Department of Biochemistry and Immunology, Cardiff and Vale University Health Board, University Hospital of Wales, Cardiff, UK and Department of Medical Biochemistry, School of Medicine, Alexandria University, Egypt; [4]Servizio Immunotrasfusionale, "A. Cardarelli" Hospital, Naples, Italy; [5]Division of Nephrology and Center for Vascular Biology Research, Beth Israel Deaconess Medical Center and Department of Medicine, Harvard Medical School, Boston, MA, USA; [6]Department of Laboratory Medicine, Boston Children's Hospital and Department of Pathology, Harvard Medical School, Boston, MA, USA; and [7]Department of Medicine, University of Verona, Italy

 doi:10.3324/haematol.2016.142372

Received: January 12, 2016.

Accepted: April 29, 2016.

Pre-published: May 5, 2016.

Correspondence: andolfo@ceinge.unina.it

Supplementary data of "Functional characterization of novel ABCB6 mutations and their clinical implications in familial pseudohyperkalemia" by Andolfo et al.

Supplementary Table S1: RMSD values of modeled mutant ABCB6 dimers superposed on modeled WT ABCB6 homodimers in both inward- and outward-facing conformations. The heterodimeric (compound heterozygous) mutant polypeptides are considered in both possible conformations, since the productive alignments for modeling of monomer "a" and monomer "b" within the dimer were of different length, as explained in Methods and Figure 1 legend.

Supplementary Table S2: Minor allele frequency of the variants identified in this study by the analysis of the public databases 1000 genomes, NHLBI Exome Sequencing Project and Exome Aggregation Consortium.

Supplementary Figure legends

Figure 1S. A. Three-dimensional structural model of a portion of homodimeric human ABCB6 DHSt mutant p.V454A in an inward-facing conformation, as modeled on the aligned structure of *M. musculus* ABCB1A (PDB ID 3G5U). Monomer "a" (blue) of the homodimer represents ABCB6 aa residues 246 (N-) to 826 (-C), modeled on transmembrane helices 1-6 and NBD-1 of ABCB1A. Monomer "b" of the homodimer (pink) represents ABCB6 aa residues 237 (N'-) to 826 (-C') modeled on ABCB1A transmembrane helices 7-12 and its NBD-2. A surface model is superposed on the modeled polypeptide backbone ribbon structure. Residue A454 (red spheres) is located between the membrane-spanning helices and the NBDs, extending into the cytoplasmic vestibule of the dimer. The cavity (cyan spheres) at the intermonomeric interface outlines a postulated intra-membrane binding site for inhibitors of ABCB6-mediated porphyrin transport[31], corresponding to the ABCB1 binding site of inhibitor QZ59[32]. Note that in this and subsequent figures, each modeled ABCB6 monomer lacks its ectofacial N-terminal tail and putative transmembrane spans 1-5, but includes putative transmembrane spans 6-11 (TM) followed by the single nucleotide-binding domain (NBD). **B.** Transverse intra-membrane profile of the modeled inward-facing conformation of homodimeric ABCB6 mutant V454A (as in panel A), with transmembrane helices rotated 90° around the axis shown. The view (lacking NBDs) looks outward from the ICL region, near the separated mutant A454 residues (red). The colored M1 domain helices are numbered 6-11 for ABCB6 monomer "a", and 6'-11' for the monomer "b" of the ABCB6 dimer. The arrows between helices 9 and 11 on one side, and helices 9' and 11' on the other side of the dimer mark the locations of side apertures proposed in mouse ABCB1 to mediate hydrophobic drug uptake from the inner

leaflet of the lipid bilayer for subsequent efflux from the cell, or for flippase-like transfer to the outer leaflet[32]. **C.** Three-dimensional structural model of homodimeric human ABCB6 mutant p.V454A in an outward-facing conformation, as modeled on the aligned structure of S. aureus Sav1866 (PDB ID 2HYD). The black oval encloses a central cavity at the inter-monomeric interface, hypothesized to be an intra-membrane substrate binding site (as predicted for homodimeric Sav1866 of S. aureus[33]). **D.** Transverse intramembranous profile of the modeled outward-facing conformation of dimeric ABCB6 (as in panel C), with the transmembrane helices rotated 90^{o} around the axis shown. The view (lacking NBDs) looks inward from the extracellular edge of the outer leaflet of the membrane bilayer towards the approximated mutant A454 residues (red) at the level of the ICL region. Helices are labeled at ends closest to reader. The figure was prepared in PyMOL.

Figure 2S. A. Three-dimensional structural model of a portion of the heterodimeric human ABCB6 compound heterozygous DHSt mutant p.R276W/p.R723Q in an inward-facing conformation (please Fig. 1 legend for details). Mutant residue W276 (magenta spheres) of monomer A is located within the lipid bilayer. Mutant residue Q723 (olive spheres) of monomer B is located within the NBD region in the cytoplasmic vestibule of the dimer. The cavity (cyan spheres) at the intermonomeric interface outlines a postulated intramembranous inhibitor binding site **B.** Transverse intra-membrane profile of the modeled inward-facing conformation of heterodimeric ABCB6 mutant p.R276W/p.R723Q (as in panel A) with transmembrane helices rotated 90° around the axis shown. The view, lacking NBDs, looks outward from the cytoplasmic edge of the inner leaflet, and includes mutant residue W276 (magenta) of monomer A, but not mutant residue Q723 of monomer B. Helical numbering and arrows are as defined in Fig. 1B. **C.** Three-dimensional structural model of a portion of the heterodimeric human ABCB6 compound heterozygous DHSt mutant p.R276W (magenta)/p.R723Q (olive) in an outward-facing conformation, as modeled on the aligned structure of *S. aureus* Sav1866 (PDB ID 2HYD). The black oval encloses a central cavity at the inter-monomeric interface (as in Fig. 1). **D.** Transverse intra-membrane profile of the modeled outward-facing conformation of heterodimeric ABCB6 p.R276W/p.R723Q (as in panel C), with the transmembrane helices rotated 90^{o} around the axis shown. The view, lacking NBDs, looks inward from the extracellular edge of the outer leaflet, highlighting mutant residue W276 protruding for the periphery of the transmembrane helical bundle. Helices are labeled at ends closest to reader. The figure was prepared in PyMOL.

Supplementary Methods

Sequencing analysis

The search for mutations was performed by direct sequencing, using 75 ng genomic DNA. All exons and flanking splice junctions of the *ABCB6* gene were amplified by PCR in a 25 µl volume with Master Mix 2X (Promega). Oligonucleotide primers were designed by the program Primer3 v.0.4.0. Primer sequences are available on request (e mail: achille.iolascon@unina.it). Integrity of PCR products was checked by agarose gel electrophoresis. Direct sequencing was performed using the BigDye® Terminator Cycle Sequencing Kit (Applied Biosystems, Branchberg, NJ, USA) and a 3730 DNA Analyzer (Applied Biosystems). Missense substitution mutations in ABCB6 (Q9NP58) were evaluated by Poly-Phen-2 (http://genetics.bwh.harvard.edu/pph2/index.shtml) and SIFT (http://sift.jcvi.org/) online tools.

Immunofluorescence analysis

HEK-293 cells ($2x10^6$) on coverslips were transfected with ABCB6 cDNAs. After 72 hrs, cells were fixed, and immunostained with anti-FLAG (1:200; F3165, Sigma) and anti-WGA (Wheat Germ Agglutinin, Alexa Fluor 555 Conjugate, Life Technologies). Secondary antibodies for FLAG (Alexa Fluor 488 goat anti-mouse; Life Technologies) were incubated at 1:200 dilution in PBS for 30 min at room temperature. Nuclei were stained with 1 µg/ml DAPI in PBS for 15 min at room temperature. The coverslips were mounted in 50% glycerol (v/v) in PBS and imaged by Zeiss LSM 510 Meta confocal microscope equipped with an oil immersion plan Apochromat 63× objective 1.4 NA, Green channel excitation of Alexa488 by the argon laser 488 nm line was detected with the 505-550 nm emission bandpass filter. Red channel excitation of Alexa546 by the Helium/Neon laser 543 nm line was detected with the 560-700 nm emission bandpass filter (using the Meta monochromator). Blue channel excitation of DAPI by the blue diode laser 405 nm line was detected with the 420-480 nm and emission bandpass filter.

Cell culture and transfection assay

Human HEK-293 cells were maintained in DMEM medium (Sigma) supplemented with 10% fetal bovine serum (FBS), 100 U/mL penicillin, and 100 mg/mL streptomycin (all from Life Technologies), in a humidified 5% CO_2 atmosphere at 37°C.

pcDNA3.1-ABCB6-WT and pcDNA3.1-ABCB6 mutant constructs (5µg) were transfected into HEK-293 cells using X-tremeGENE HP DNA Transfection Reagent (Roche, Indianapolis, IN, USA). To phenocopy the heterozygous genotypes, cells were transfected with 2.5µg of WT

pcDNA3.1-ABCB6-WT plus 2.5µg of pcDNA3.1-ABCB6 mutants R375Q, p.R276W or R375W. For the compound heterozygous genotypes, cells were transfected with 2.5µg pcDNA3.1-ABCB6-R276W plus 2.5µg pcDNA3.1-ABCB6-R723Q. For the homozygous genotype, cells were transfected with 5µg pcDNA3.1-ABCB6-V454A. After 72 hrs, cells were harvested for analysis.

Exome capture and sequencing

Blood was obtained for genetic analysis from affected and unaffected family members of the Irish family and from healthy controls, with signed informed consent according to the Declaration of Helsinki. Blood collection was according to protocols approved by local university ethics committees. Genomic DNA was prepared from peripheral blood with the Wizard Genomic DNA purification kit (Promega, Milano, Italy). 5µg of DNA from two affected and two unaffected members of DHSt family Edinburgh was diluted in 700 µl of Nebulization buffer (Illumina, San Diego, CA) and sheared by nebulizers (Invitrogen, Carlsbad, CA) into fragments of 200–400 bp in length (Bioanalyzer 2100, Agilent, Santa Clara, CA). Sheared samples purified by QIAquick spin columns (Qiagen, Hilden, Germany) were processed for library preparation (Illumina protocol), omitting size-selection of adapter-ligated fragments prior to capture. After several cycles of PCR amplification, 500 ng of DNA from the resulting libraries was hybridized to the bait set from the SureSelect Human All Exon Kit (Agilent, Santa Clara, CA, USA) at 65°C for 24 h. Hybrid capture with streptavidin-coated Dynal magnetic beads (Invitrogen, Carlsbad, CA) was performed as manufacturer's protocol. Captured samples were further purified through Agencourt AMPure XP beads and subjected to PCR amplification. All samples at each step of library preparation were quantified by Bioanalyzer 2100 (Agilent). Individual sample libraries were NaOH-denatured and loaded onto one lane of an Illumina Flowcell v4. DNA clusters were generated through a one-step workflow on the Cluster Station using TruSeq PE Cluster Kit v5 (Illumina, San Diego, CA). A PhiX control library added to each sample at 1% volume served as internal control. Sequencing was performed on the Illumina Genome Analyzer IIx platform as paired-end 100-bp reads according to the manufacturer's protocol. An exome capture was considered successful if >80% of the target regions were covered with a high quality genotype.

Reads were aligned to the most recent version of human genome (GRCh37/hg19) using the BWA software package v0.5.9.

Molecular cloning of ABCB6 and Site-directed mutagenesis

To detect and determine the inheritance pattern of the two mutations in patient Cardiff 2, the DNA fragment encompassing the two mutations R276W and R723Q, of ABCB6 was PCR-amplified and cloned into PCR Cloning Vector pSC-A-amp/kan (StrataClone PCR Cloning Kit, Agilent). Point mutations c.1123 C>T, p.R375Q; c.1361T>C; p.V454A; c.826G>T; p. R276W; c.2168G>A; p.R723Q; c.1124 G>A; p.R375W were introduced into pcDNA3.1-ABCB6 with the QuikChange kit (Stratagene, La Jolla, CA). The integrity of the complete ABCB6 coding region was confirmed by sequencing after mutagenesis. Primers sequences are available upon request.

RNA isolation, cDNA preparation and quantitative qRT-PCR

Total RNA was extracted from cell lines and peripheral blood samples from patients and healthy controls using Trizol reagent (Life Technologies). Synthesis of cDNA from total RNA (2 μg) was performed using Super Script II First Strand kits (Life Technologies). Quantitative RT-PCR (qRT-PCR) was by the SYBR-green method using the ABI PRISM 7900HT Sequence Detection system. Relative gene expression was calculated using the $2^{(-\Delta Ct)}$ method, where ΔCt indicates the differences in the mean Ct between selected genes and the internal control (GAPDH or β-actin). Sequences of the qRT-PCR primers designed for each gene using Primer Express 2.0 (Life Technologies) are available upon request.

Immunoblotting

Total cell lysates (80 μg protein) electrophoresed on SDS-polyacrylamide gels were electroblotted onto polyvinylidene difluoride membranes (BioRad, Milan, Italy), incubated with the following antibodies: anti-FLAG (1:500; F3165, Sigma), anti-β-actin antibody (1:1000; Sigma, used as loading control), then imaged with HRP-conjugated anti-rabbit Ig (1:5000) (GE Healthcare, UK) and enhanced chemiluminescence substrate (Supersignal West Pico Chemiluminescent Substrate Kit, ThermoScientific, Miami USA). Labeled bands were visualized and densitometric analysis performed with the BioRad Chemidoc using Quantity One software (BioRad).

Statistical analysis

Data are presented as means ± standard error of the mean (s.e.m.). Statistical significance was calculated using the Mann-Whitney test and Student's t test. Correlation analysis was calculated using Spearman's rank correlation coefficient and Pearson's correlation coefficient. $P < 0.05$ was considered as statistically significant.

Table S1. RMSD values (Å) of homology-modeled structures of WT and mutant ABCB6 homodimers superposed on modeled WT and other mutant ABCB6 dimer structures

	homozygous			compound heterozygous	
	p.V454A	p.R276W	p.R723Q	p.R276W/R723Q(chainA)	p.R276W/R723Q(chainB)
WT	1.48 (0.81)	0.98 (0.29)	1.17 (0.79)	1.88 (0.58)	1.57 (0.74)
p.V454A	-	1.66 (0.84)	1.41 (0.97)	1.07 (0.87)	0.69 (0.93)
p.R276W	-	-	1.59 (0.83)	2.00 (0.59)	1.52 (0.79)
p.R723Q	-	-	-	1.96 (0.64)	1.61 (0.43)

Table S2. Minor allele frequency of the *ABCB6* variants

Database	**Population**	**MAF (C) rs61733629** (c.1361T>C; p.V454A)	**MAF (T) rs57467915** (c.826G>T; p.R276W)	**MAF (A) rs148211042** (c.2168G>A; p.R723Q)
1000 Genomes	AFR	0/1322	1/1322	0/1322
	AMR	28/694	2/694	0/694
	EAS	1/1008	0/1008	0/1008
	EUR	0/1006	15/1006	1/1006
	SAS	0/978	1/978	0/978
	ALL	**29/5008; 0.58%**	**19/5008; 0.38%**	**1/5008; 0.02%**
NHLBI Exome Sequencing Project	ESP6500:European_American	2/8600	114/8600	9/8600
	ESP6500:African_American	2/4406	17/4406	2/4406
	ALL	**4/13006; 0.03%**	**131/13006; 1%**	**11/13006; 0.08%**
Exome Aggregation Consortium (ExAC)	**ALL**	**556/121256; 0.46%**	**632/33350; 1.9%**	**101/118464; 0.09%**
Total count		**618/144278; 0.43%**	**782/51364; 1.5%**	**113/136478; 0.08%**

Figure 1S: Andolfo et al. 2015

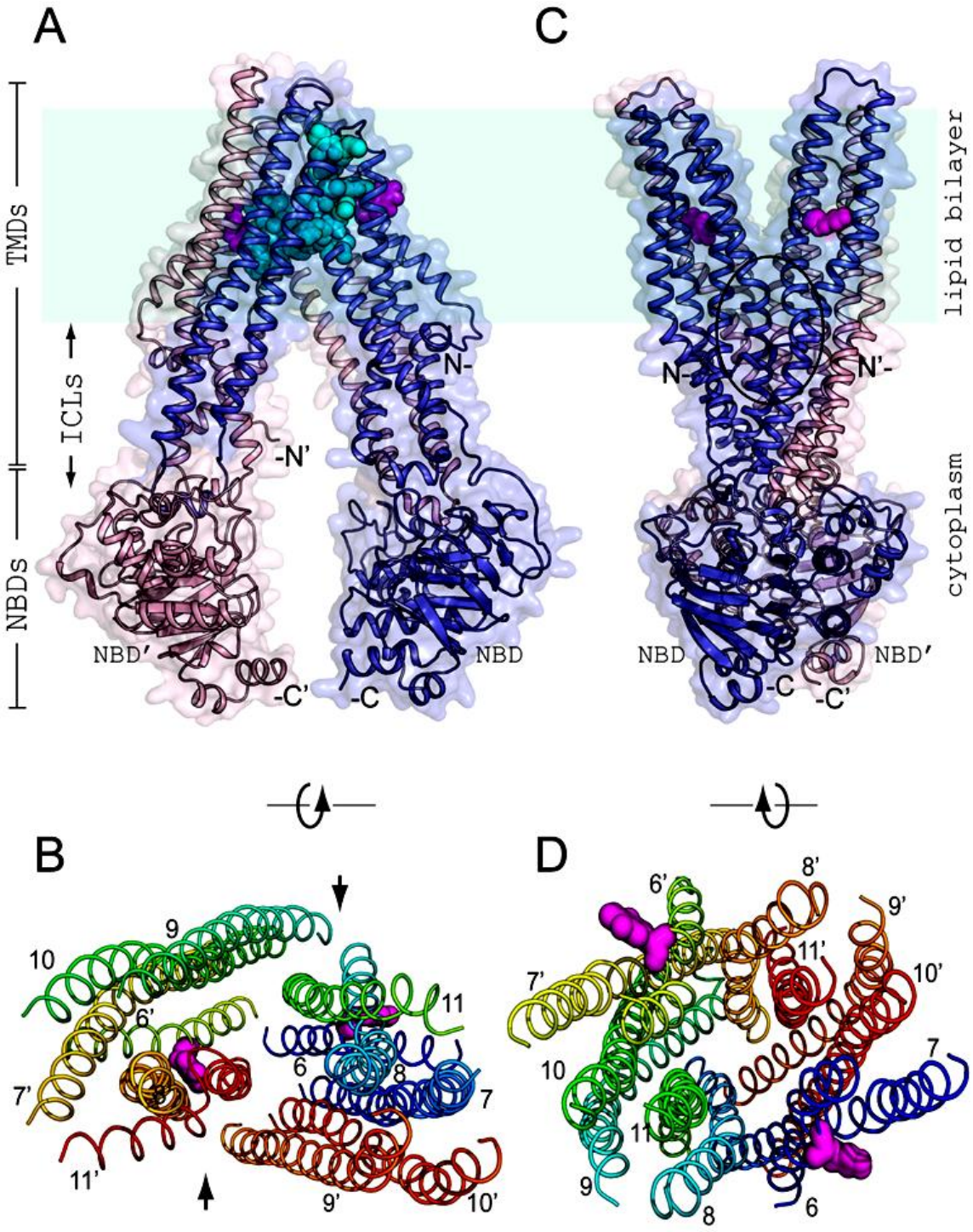

Figure 2S. Andolfo et al. 2015